Supplementary Table

Table S1

Region	P-region	A-region	Interaction Type
R1	U2074	G2597	cSS
	C2073:G2436	A2598	A-minor
R2	*C2463	*A2518	Hydrogen Bonding
	G2489		
R3	A2060	G2502	Base Stacking
	A2058	A2503	Base Stacking
	A2059		
	G2061		
	C2063		
R4	A2439	A2600	Hydrogen Bonding
R5	A2453	A2572	Hydrogen Bonding
	U2491	G2570	Hydrogen Bonding
R6	G2447	U2504	cHH
	C2452	U2504	cWW

Table S1. Six RNA/RNA conserved regions of interaction within the SymR as reported by Rivas and Fox (2020). Ribonucleotides from the P- and A-region involved in each case are listed. *Thermus thermophilus* numbering system is used. Non-standard and standard base pair interactions are described using the Leontis-Westhof classification (Leontis and Westhof, 2001). A-minor and Base stacking motives were determined using DSSR software (Lu *et al.*, 2005) as reported by the authors. Single hydrogen bonding as reported by Rivas and Fox (2020). * C2463 and A2518 are left out of tt_A1P1 construct, therefore interaction region 2 is no longer possible.

Supplementary Figures

Figure S1

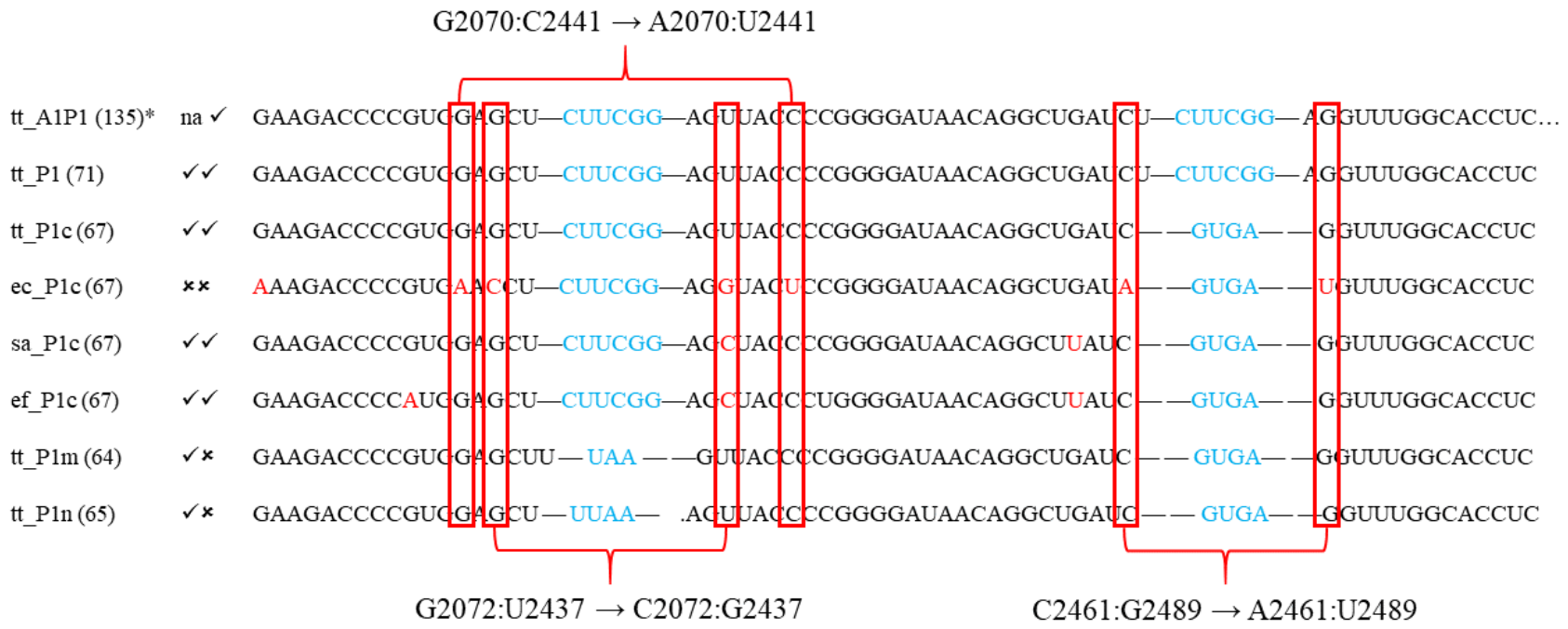

Figure S1. Sequence alignment representation of the P-region based constructs. tt_A1P1 construct also includes the A-region sequence but was deleted for this alignment to focus on its P-region part. The length of each construct in ribonucleotides is placed between brackets in front of each construct code. Their ability to form dimers and produce a peptide bond in each case is marked by an ✓ or an × in each row respectively. Sequence changes are highlighted using red fonts. *Thermus thermophilus* numbering system is used. Two differences were found in the ec_P1c construct in H74, pair G2070:C2441 is replaced by A2070:U2441 and the pair G2072:U2437 is replaced by C2072:G2437. One difference on the same construct was also found in H89, the pair C2461:G2489 is replaced by A2461:U2489. These changes are marked using red boxes. The sequences used at the tip of H74 and H89 respectively are highlighted using a light-blue font.

Figure S2

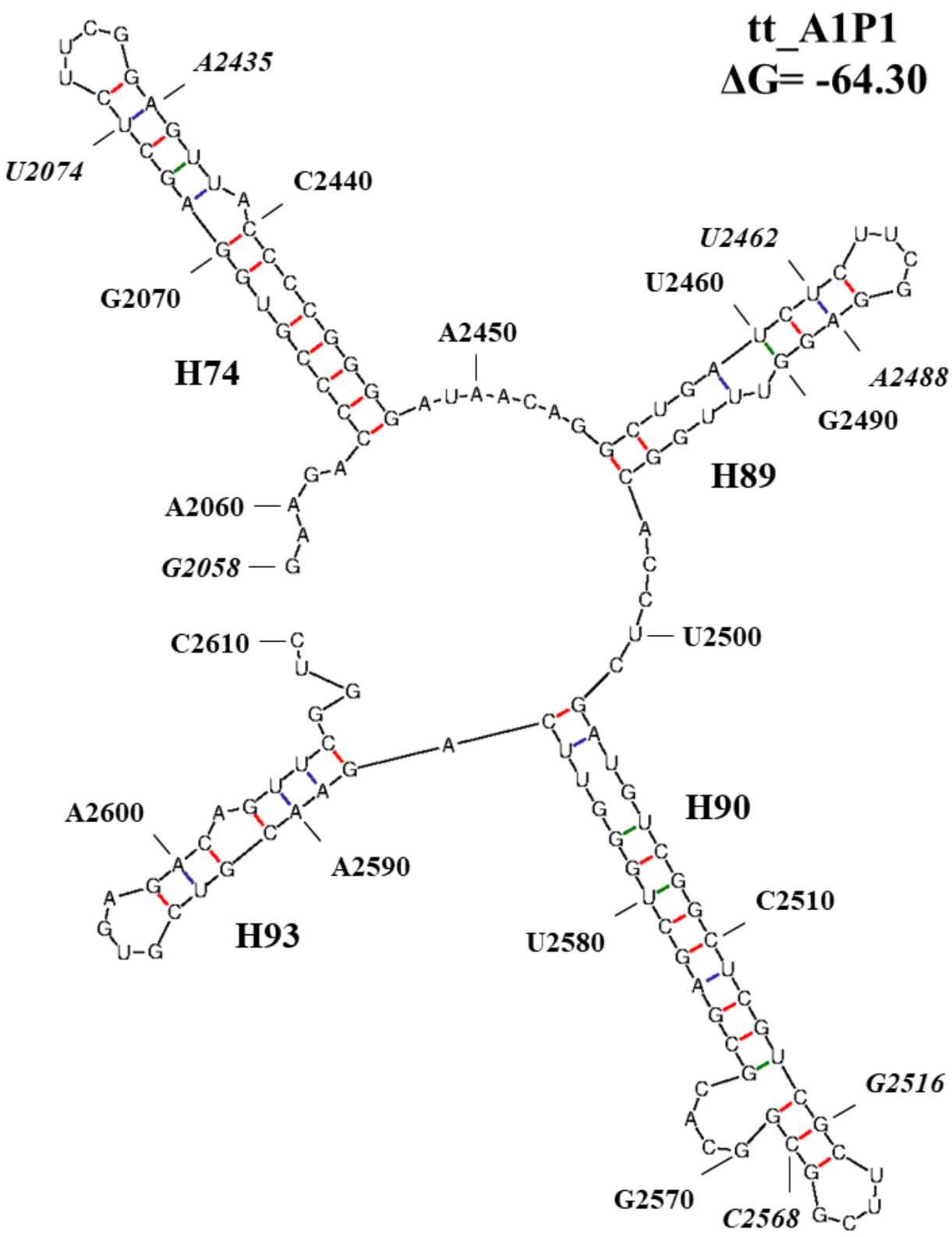
tt_A1P1
ΔG= -64.30
A2435
U2074
C2440
G2070
H74
A2450
U2462
U2460
A2488
G2490
H89
A2060
G2058
C2610
U2500
A2600
A2590
H93
H90
C2510
U2580
G2516
G2570
C2568

Figure S2. Secondary structure of the tt_A1P1 construct predicted by mfold (Zuker, 2003). With a ΔG of -64.30 Kcal/mol. *Thermus thermophilus* numbering system is used. According to this prediction base paring shift occur in H74, H89 and H90. The overall shape of H90 has grown by at least three base pairs at the beginning of the helix compared to the secondary structure of the extant ribosome.

Figure S3

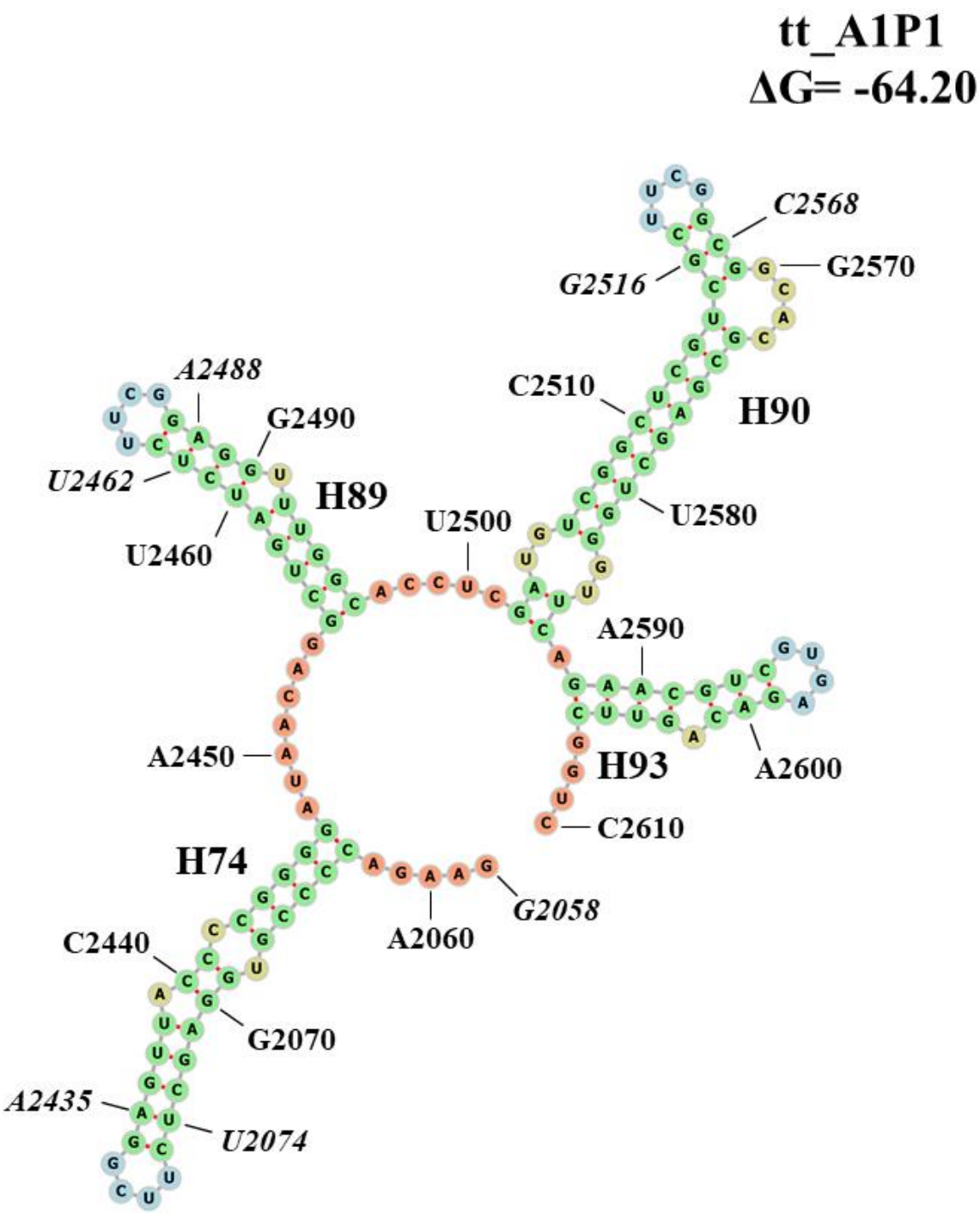
tt_A1P1
ΔG= -64.20
C2568
G2516
G2570
A2488
G2490
C2510
H90
U2462
H89
U2580
U2500
U2460
A2590
A2450
H93
A2600
C2610
H74
G2058
A2060
C2440
G2070
A2435
U2074

Figure S3. Secondary structure of the tt_A1P1 construct predicted by RNAfold (Gruber *et al.*, 2008). With a ΔG of -64.20 Kcal/mol. *Thermus thermophilus* numbering system is used. According to this prediction base paring shift occur in H74, H89 and H90. The overall shape of H90 has grown by at least three base pairs at the beginning of the helix compared to the secondary structure of the extant ribosome.

Figure S4

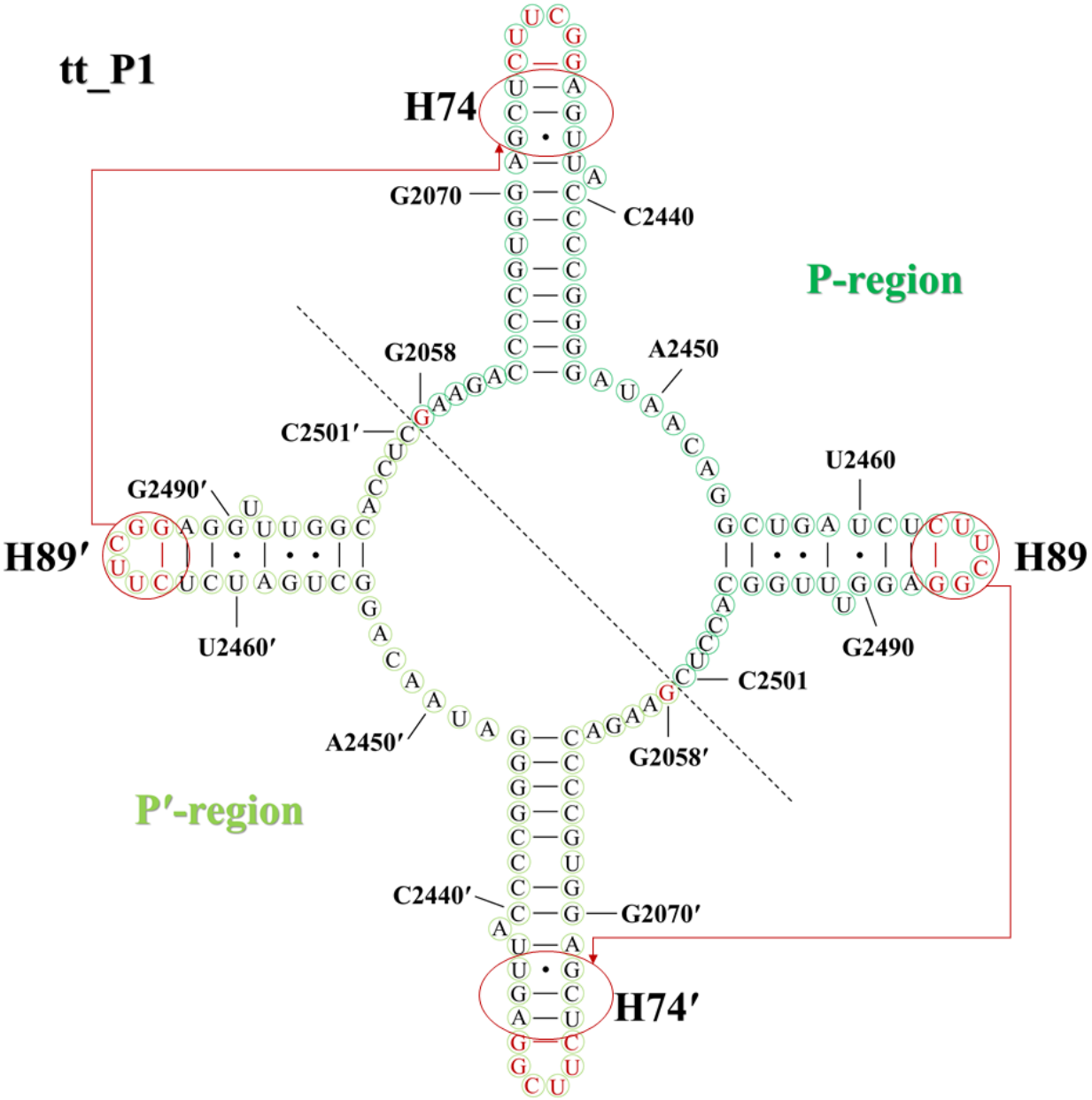
tt_P1
H74
G2070
C2440
P-region
G2058
A2450
C2501′
G2490′
U2460
H89′
H89
U2460′
G2490
C2501
A2450′
G2058′
P′-region
C2440′
G2070′
H74′

Figure S4. Secondary structure representation of the tt_P1 homodimer. Possible regions of interaction that allow hybridization are highlighted in red circumferences and connected through red arrowed lines. These regions broadly resemble regions of RNA/RNA interaction 1 and 4 as described by Rivas and Fox (2020) (Table S1). *Thermus thermophilus* numbering system is used.

Figure S5

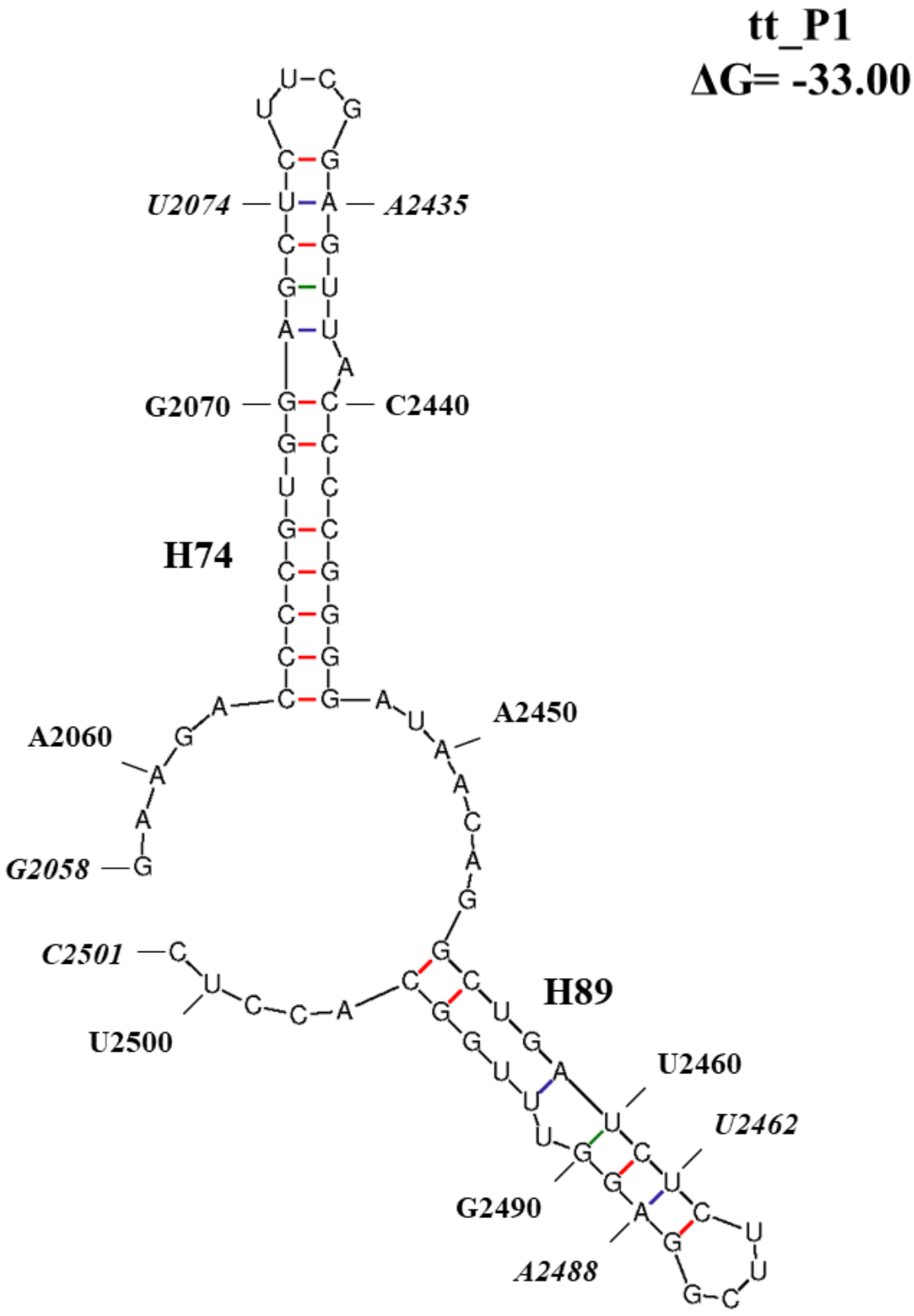
tt_P1
ΔG= -33.00
U2074
A2435
G2070
C2440
H74
A2060
A2450
G2058
C2501
U2500
H89
U2460
U2462
G2490
A2488

Figure S5. Secondary structure of the tt_P1 construct predicted by mfold (Zuker, 2003). With a ΔG of -33.00 Kcal/mol. *Thermus thermophilus* numbering system is used. H74 and H89 present a different base pairing arrangement compared to their native fold in extant *T. thermophilus* LSU (Figure 1). G2069 is now base paired with C2441 and G2070 now base pairs with C2440. G2458 base pairs with U2493 and A2459 now base pairs with U2492. These new base pairs create longer helixes with less splayed-apart elements.

Figure S6

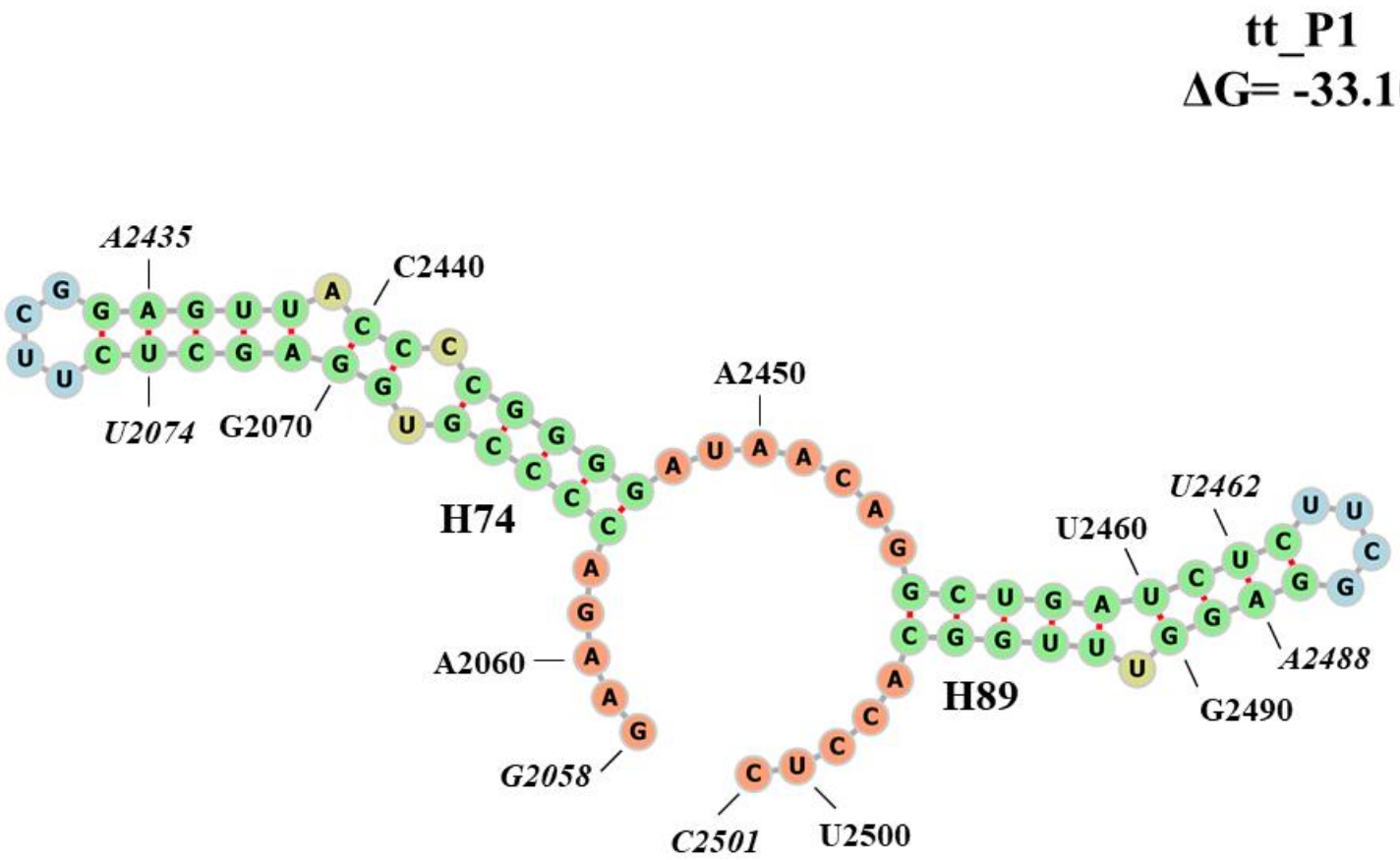
tt_P1
ΔG= -33.10
A2435
C2440
A2450
U2462
U2460
H74
H89
A2060
A2488
G2490
G2058
C2501
U2500
U2074
G2070

Figure S6. Secondary structure of the tt_P1 construct predicted by RNAfold (Gruber *et al.*, 2008). With a ΔG of -33.10 Kcal/mol. *Thermus thermophilus* numbering system is used. Same new pattern of H74 and H89 base pairing as in Figure S5.

Figure S7

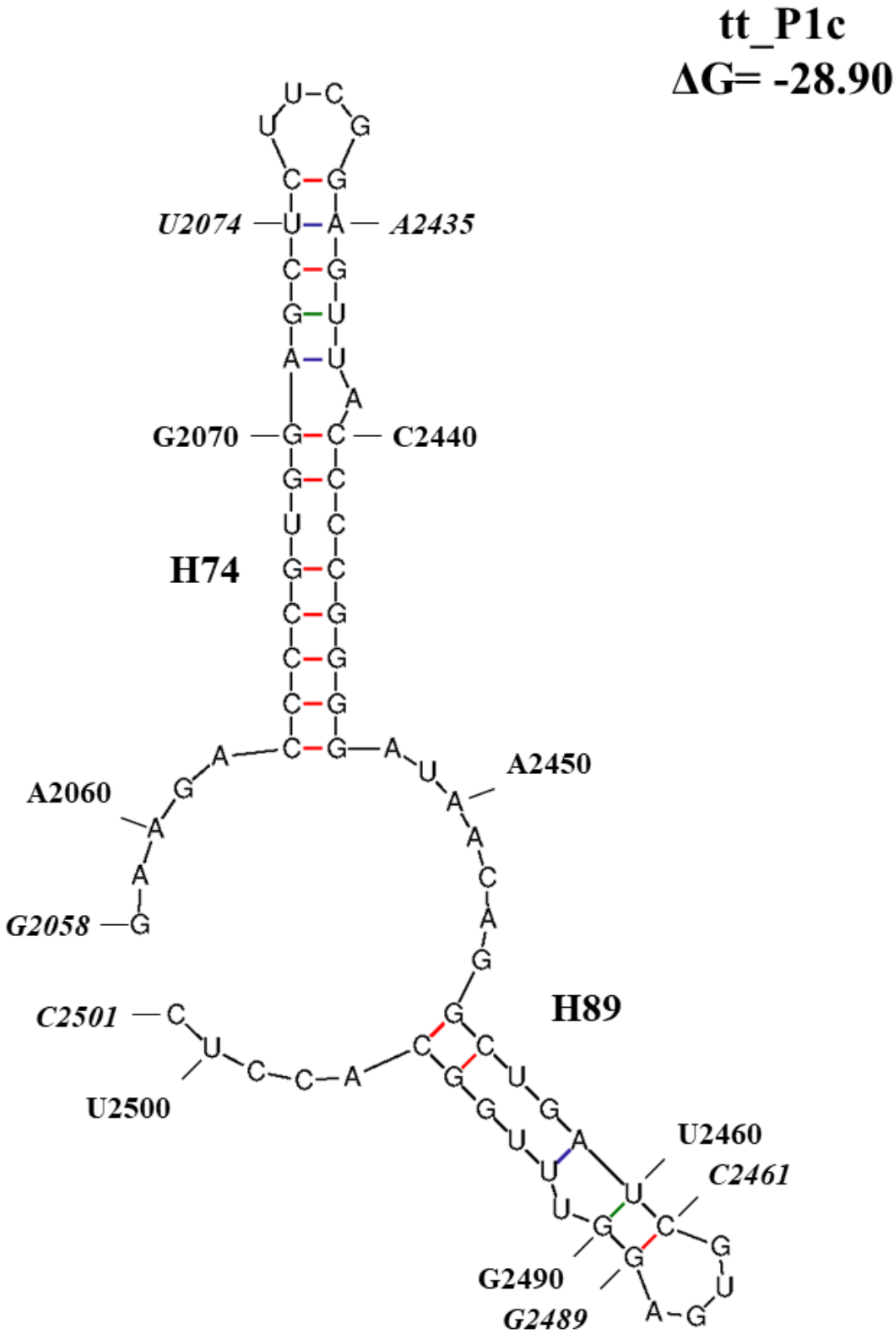
tt_P1c
ΔG= -28.90
U2074
A2435
G2070
C2440
H74
A2450
A2060
G2058
C2501
U2500
H89
U2460
C2461
G2490
G2489

Figure S7. Secondary structure of the tt_P1c construct predicted by mfold (Zuker, 2003). With a ΔG of -28.90 Kcal/mol. *Thermus thermophilus* numbering system is used. New H74 and H89 base pairing as in Figure S5 is also predicted. tt_P1 and tt_P1c differ from each other in the closing sequence of H89. The 5′-CUUCGG-3′ sequence was replaced by the 5′-GUGA-3′ as discussed in the main text.

Figure S8

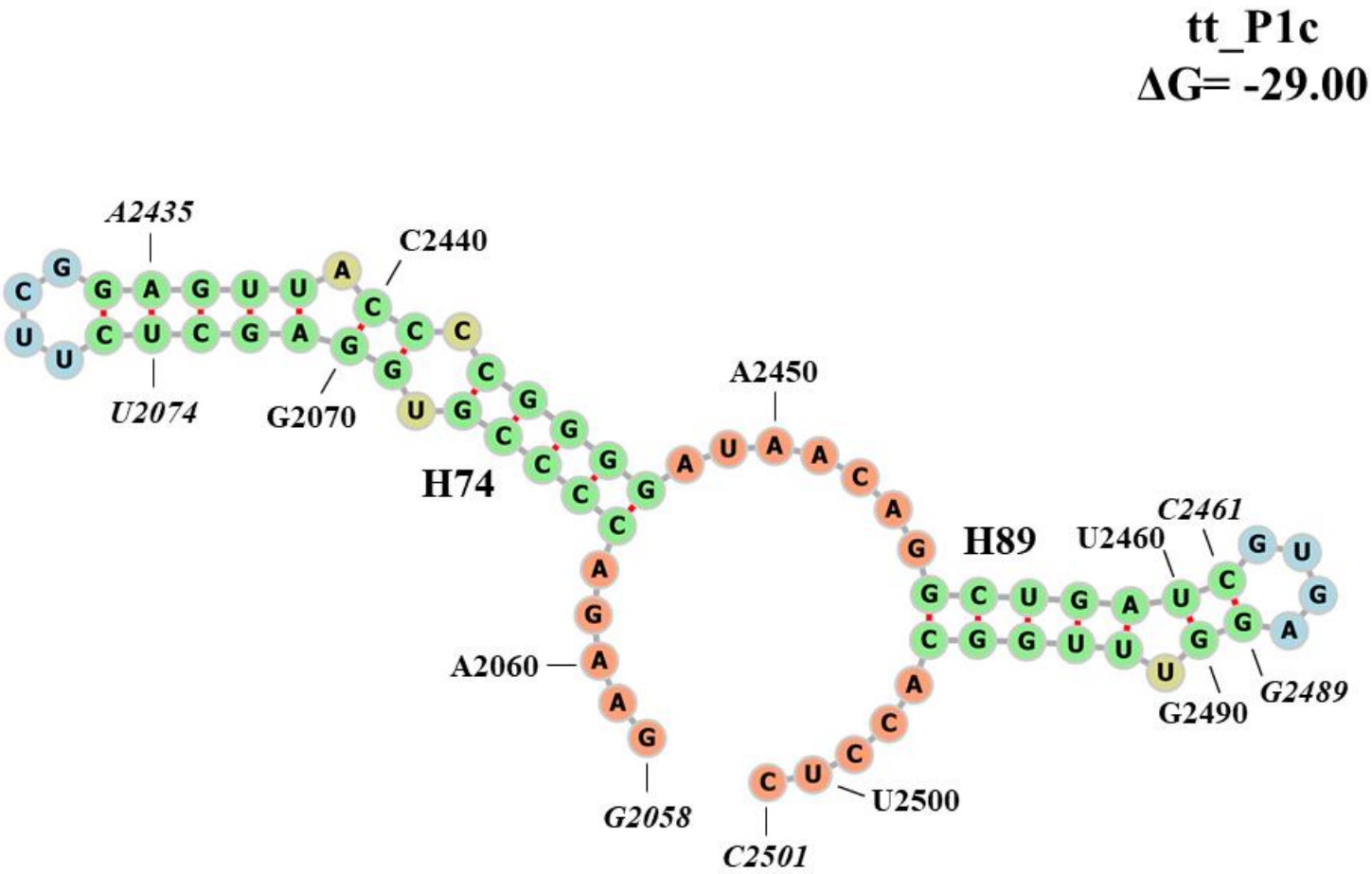
tt_P1c
ΔG= -29.00
A2435
C2440
U2074
G2070
H74
A2450
H89
C2461
U2460
G2489
G2490
A2060
G2058
U2500
C2501

Figure S8. Secondary structure of the tt_P1c construct predicted by RNAfold (Gruber *et al.*, 2008). With a ΔG of -29.00 Kcal/mol. *Thermus thermophilus* numbering system is used. Same new pattern of H74 and H89 base pairing as in Figure S5. tt_P1 and tt_P1c differ from each other in the closing sequence of H89. The 5′-CUUCGG-3′ sequence was replaced by the 5′-GUGA-3′ as discussed in the main text.

Figure S9

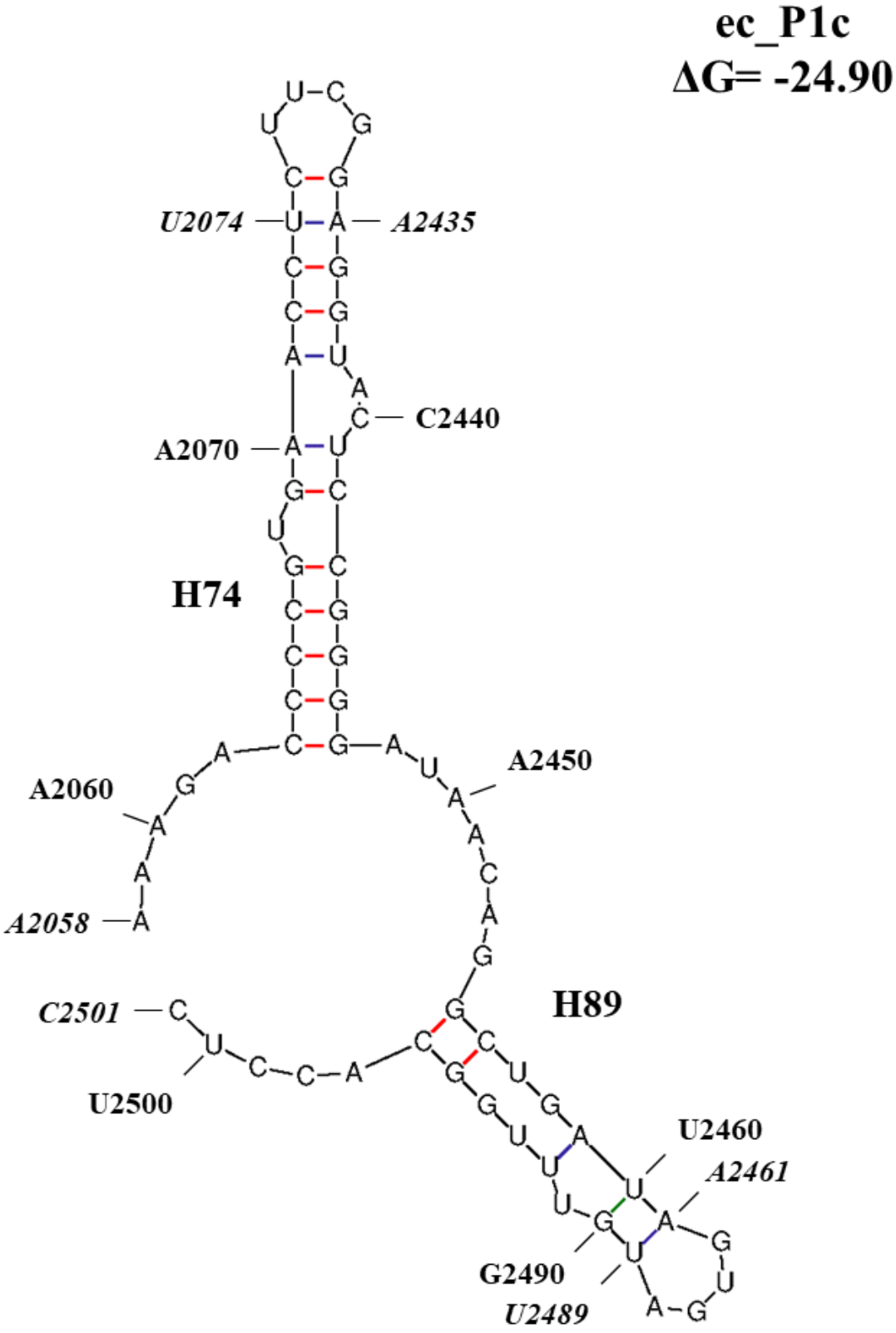
ec_P1c
ΔG= -24.90
U2074
A2435
C2440
A2070
H74
A2450
A2060
A2058
C2501
H89
U2500
U2460
A2461
G2490
U2489

Figure S9. Secondary structure of the ec_P1c construct predicted by mfold (Zuker, 2003). With a ΔG of -24.90 Kcal/mol. *Thermus thermophilus* numbering system is used. Native base pairing pattern for H74 is predicted. While new H89 pattern described in Figure S5 is also predicted.

Figure S10

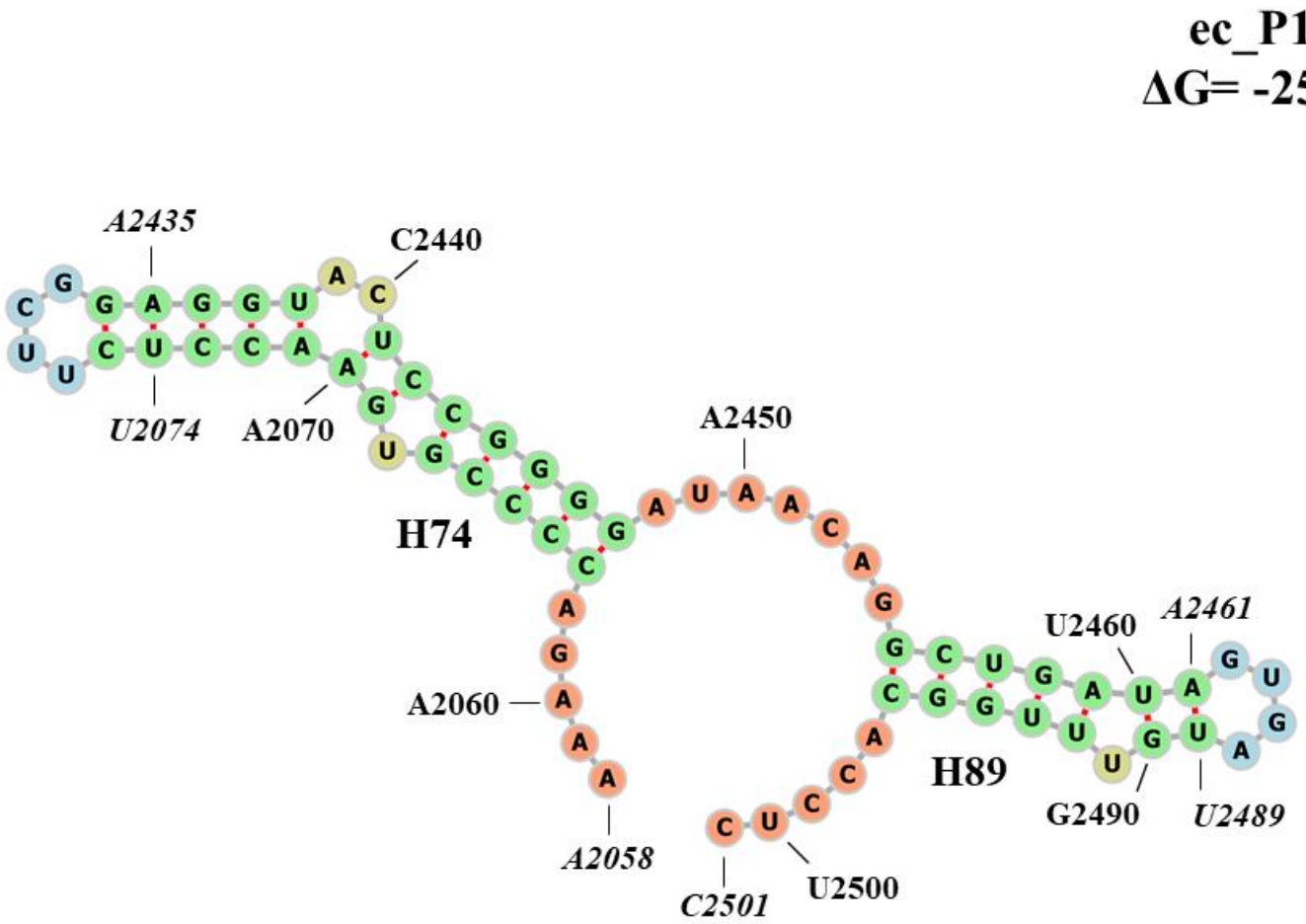
ec_P1c
ΔG= -25.00
A2435
C2440
U2074
A2070
A2450
H74
A2060
A2058
C2501
U2500
U2460
A2461
H89
G2490
U2489

Figure S10. Secondary structure of the ec_P1c construct predicted by RNAfold (Gruber *et al.*, 2008). With a ΔG of -25.00 Kcal/mol. *Thermus thermophilus* numbering system is used. Native base pairing pattern for H74 is predicted. While new H89 pattern described in Figure S5 is also predicted.

Figuere S11

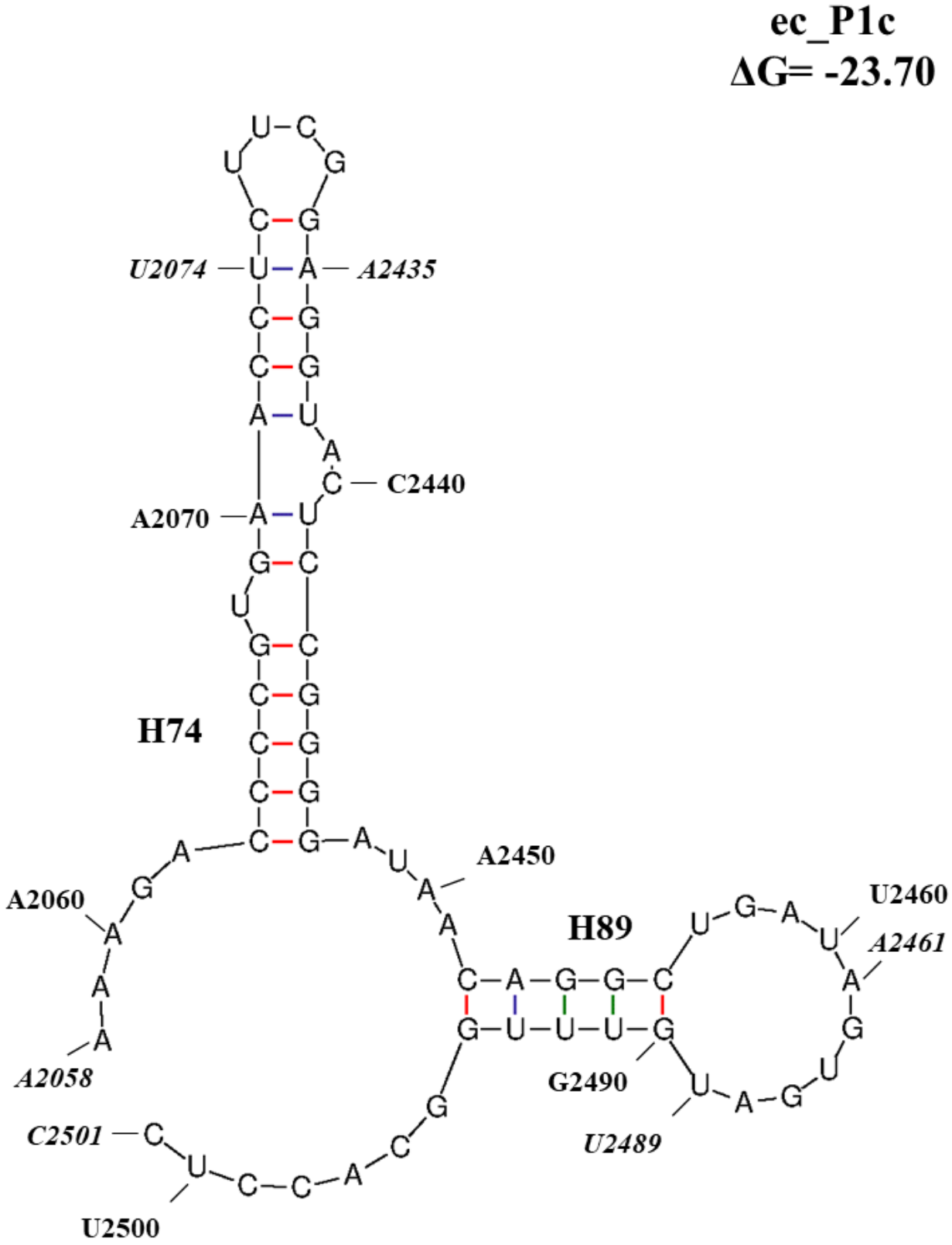
ec_P1c
ΔG= -23.70
U2074
A2435
C2440
A2070
H74
A2450
A2060
H89
U2460
A2461
A2058
G2490
C2501
U2489
U2500

Figure S11. Alternative secondary structure of the ec_P1c construct predicted by mfold (Zuker, 2003). With a ΔG of -23.70 Kcal/mol. *Thermus thermophilus* numbering system is used. Native base pairing pattern for H74 is predicted. While a new base pair arrangement is predicted for H89. C2452, A2453 and G2454 are predicted to be integrated into the helical part of H89 as well as G2455 and C2456 that now base pair with G2494, U2493, U2492, U2491 and G2490 respectively.

Figure S12

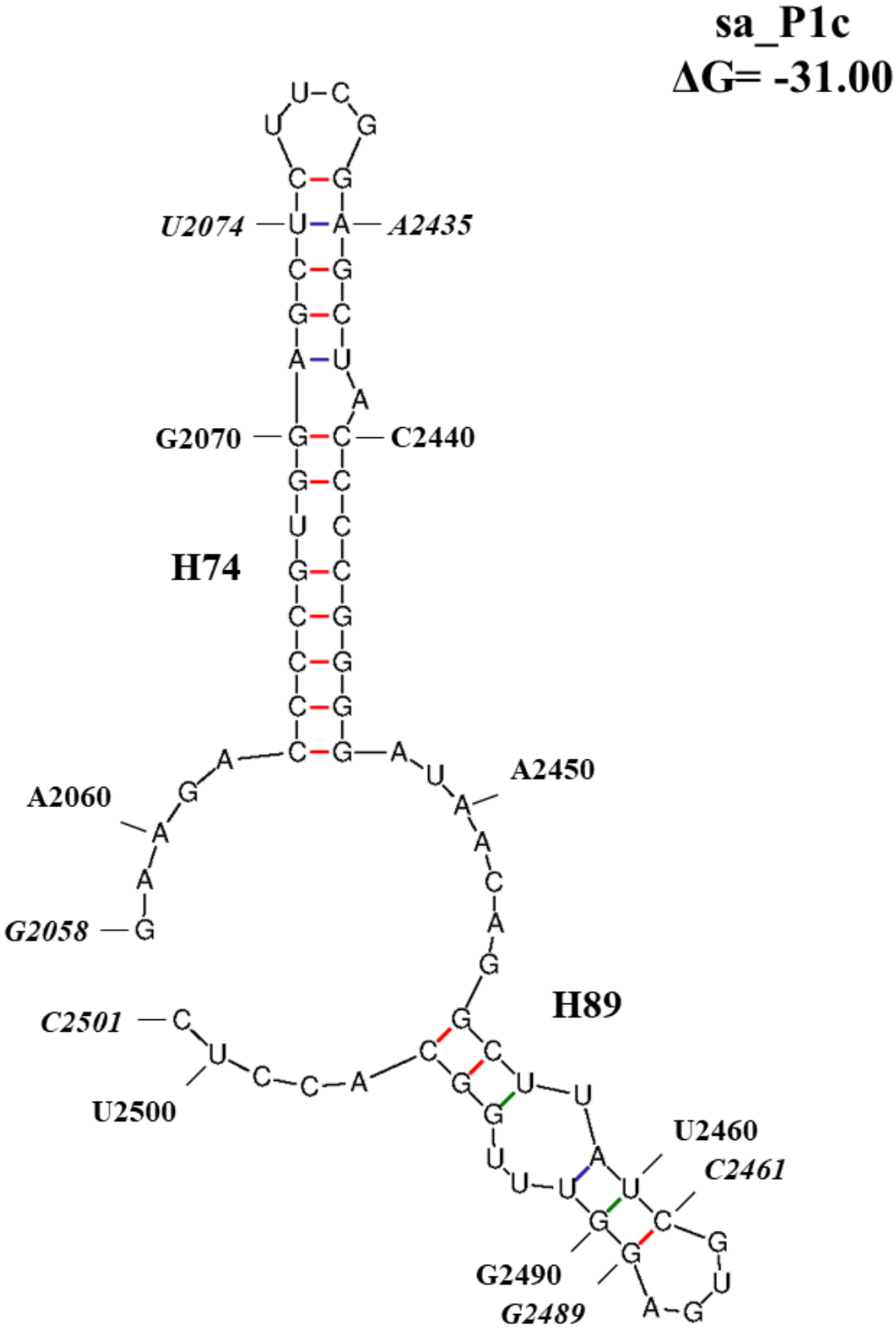
sa_P1c
ΔG= -31.00
U2074
A2435
G2070
C2440
H74
A2060
A2450
G2058
C2501
U2500
H89
U2460
C2461
G2490
G2489

Figure S12. Secondary structure of the sa_P1c construct predicted by mfold (Zuker, 2003). With a ΔG of -31.00 Kcal/mol. *Thermus thermophilus* numbering system is used. H74 is formed by the same base pairs described in Figure S5 but the shape of H89 is affected by the replacement of G2458 by U2458 creating a small bulge in the middle of the helix.

Figure S13

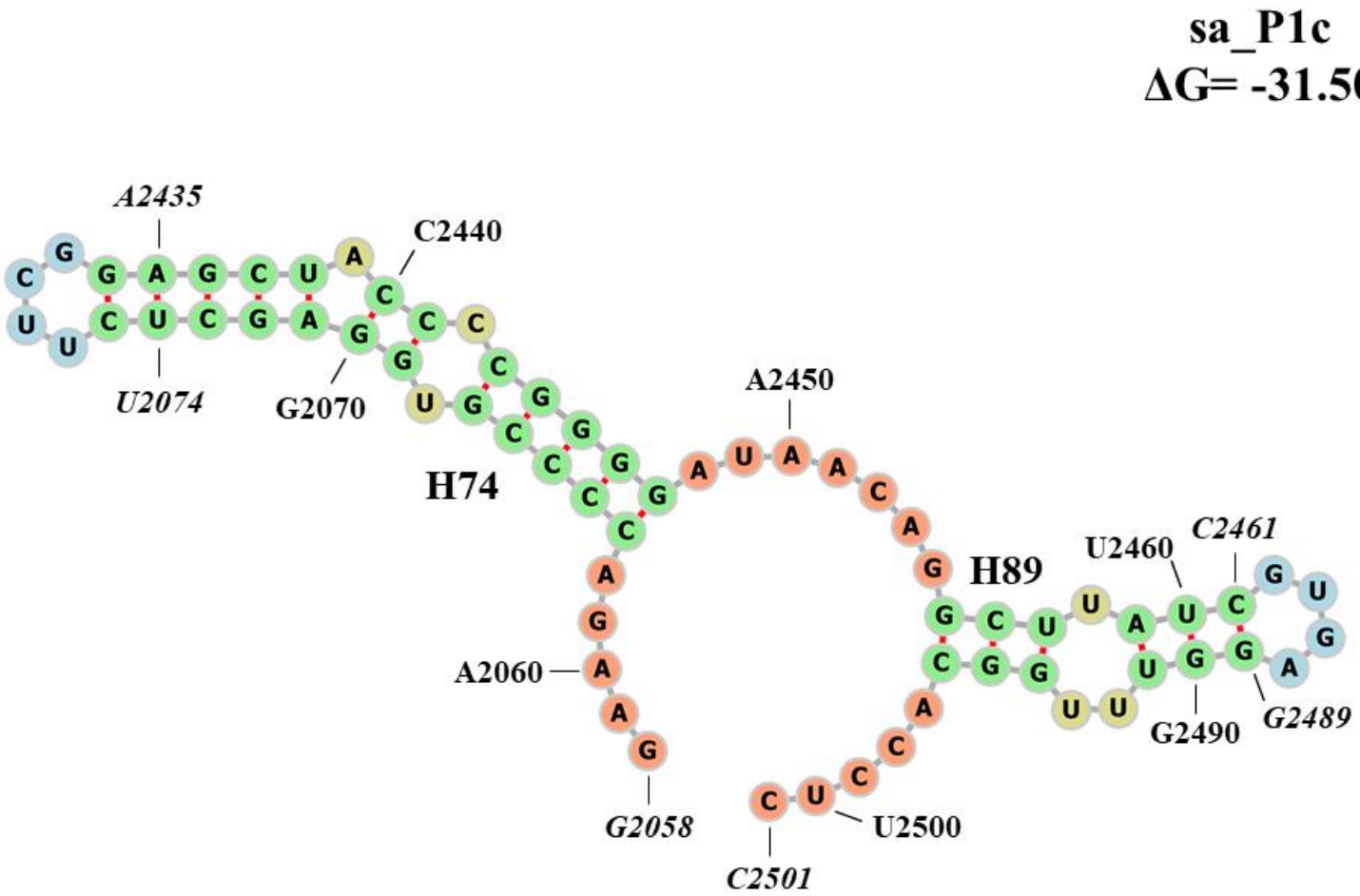
sa_P1c
ΔG= -31.50
A2435
C2440
U2074
G2070
H74
A2450
A2060
G2058
H89
U2460
C2461
G2490
G2489
C2501
U2500

Figure S13. Secondary structure of the sa_P1c construct predicted by RNAfold (Gruber *et al.*, 2008). With a ΔG of -31.50 Kcal/mol. *Thermus thermophilus* numbering system is used. H74 is formed by the same base pairs described in Figure S5 but the shape of H89 is affected by the replacement of G2458 by U2458 creating a small bulge in the middle of the helix.

Figure S14

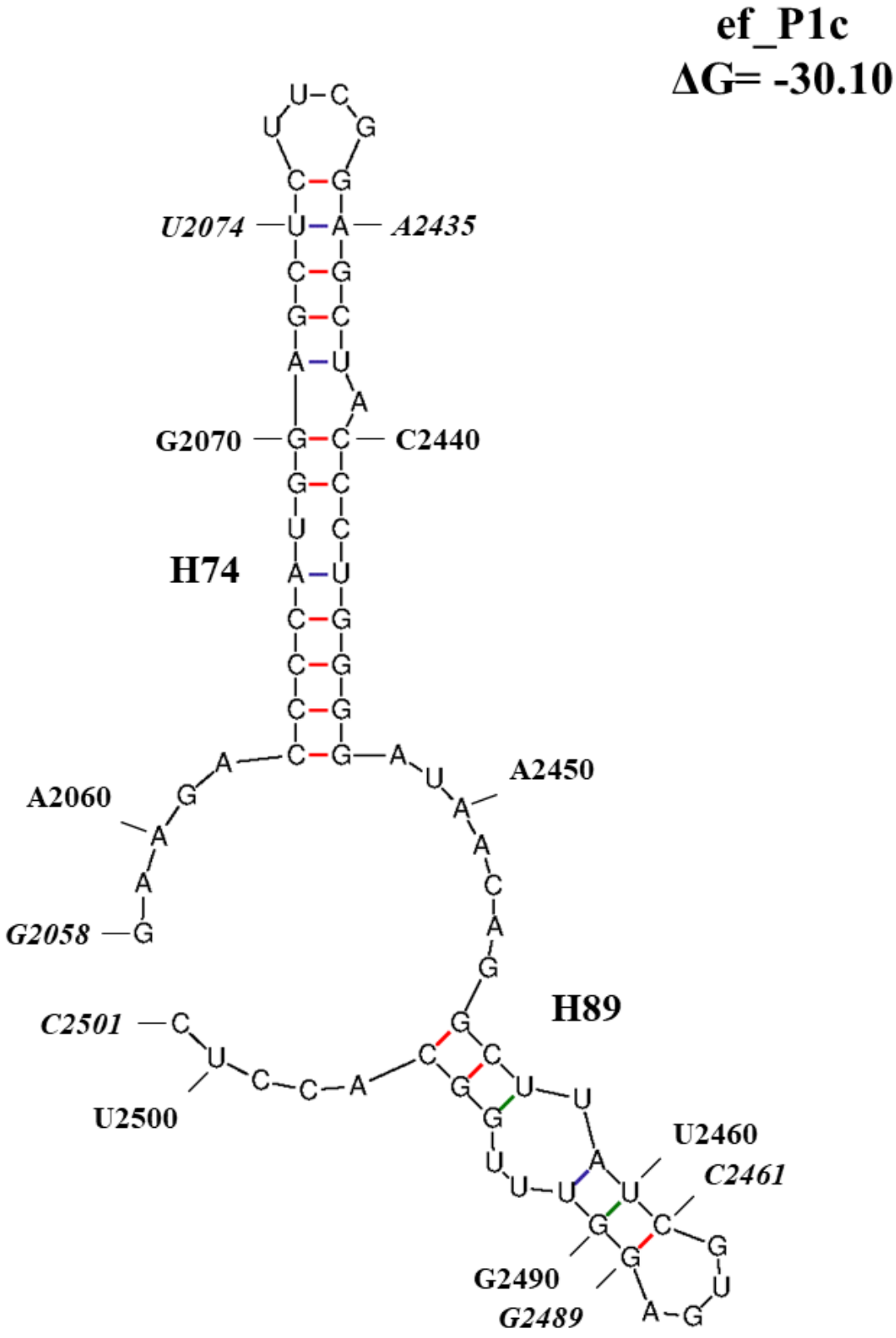
ef_P1c
ΔG= -30.10
U2074
A2435
G2070
C2440
H74
A2060
A2450
G2058
C2501
U2500
H89
U2460
C2461
G2490
G2489

Figure S14. Secondary structure of the ef_P1c construct predicted by mfold (Zuker, 2003). With a ΔG of -30.10 Kcal/mol. *Thermus thermophilus* numbering system is used. H74 and H89 share the same shape as in Figure S12.

Figure S15

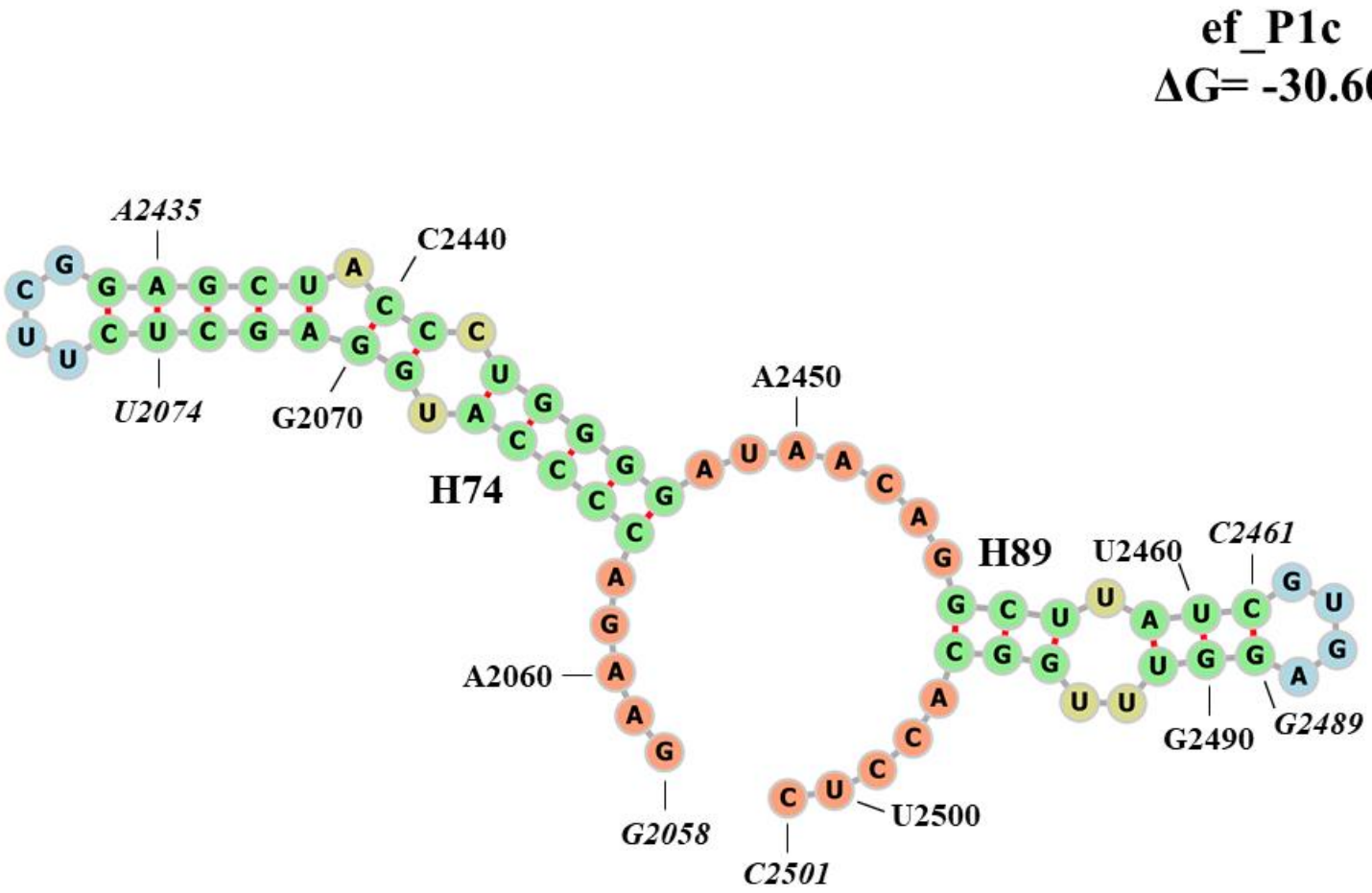
ef_P1c
ΔG= -30.60
A2435
C2440
U2074
G2070
H74
A2450
H89
U2460
C2461
A2060
G2058
C2501
U2500
G2490
G2489

Figure S15. Secondary structure of the ef_P1c construct predicted by RNAfold (Gruber *et al.*, 2008). With a ΔG of -30.60 Kcal/mol. *Thermus thermophilus* numbering system is used. H74 and H89 share the same shape as in Figure S13.

Figure S16

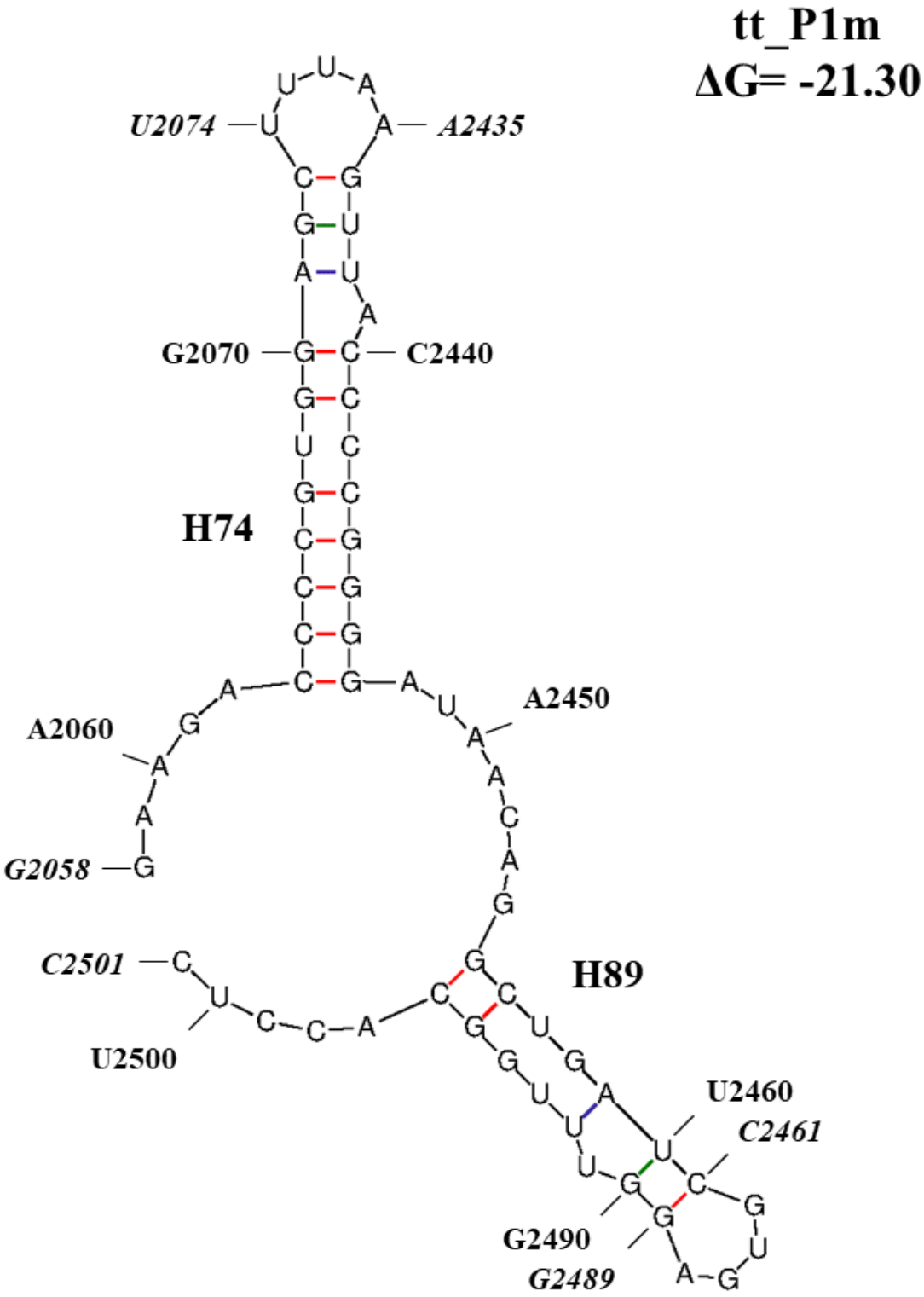
tt_P1m
ΔG= -21.30
U2074
A2435
G2070
C2440
H74
A2060
A2450
G2058
C2501
U2500
H89
U2460
C2461
G2490
G2489

Figure S16. Secondary structure of the tt_P1m construct predicted by mfold (Zuker, 2003). With a ΔG of -21.30 Kcal/mol. *Thermus thermophilus* numbering system is used. Shapes of H74 and H89 are the same as described in Figure S5. tt_P1c and tt_P1m differ in the replacement of 5′-CUUCGG-3′ by the 5′-UUA-3′ as the closing element at the tip of H74. The implications of this change are discussed in the main text.

Figure S17

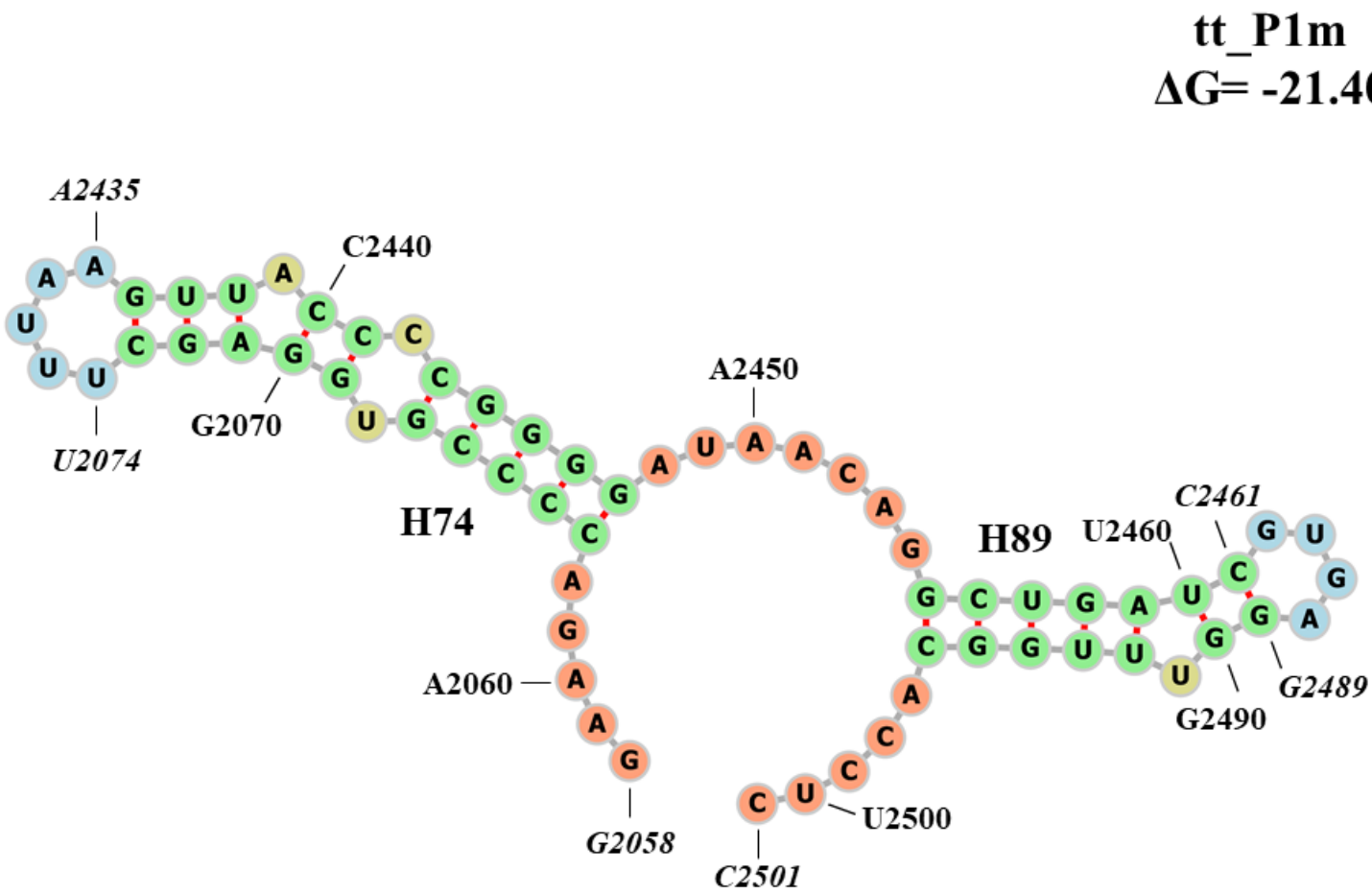
tt_P1m
ΔG= -21.40
A2435
C2440
G2070
U2074
H74
A2450
H89
U2460
C2461
G2489
G2490
A2060
G2058
U2500
C2501

Figure S17. Secondary structure of the tt_P1m construct predicted by RNAfold (Gruber *et al.*, 2008). With a ΔG of -21.40 Kcal/mol. *Thermus thermophilus* numbering system is used. Shapes of H74 and H89 are the same as described in Figure S5. tt_P1c and tt_P1m differ in the replacement of 5′-CUUCGG-3′ by the 5′-UUA-3′ as the closing element at the tip of H74. The implications of this change are discussed in the main text.

Figure S18

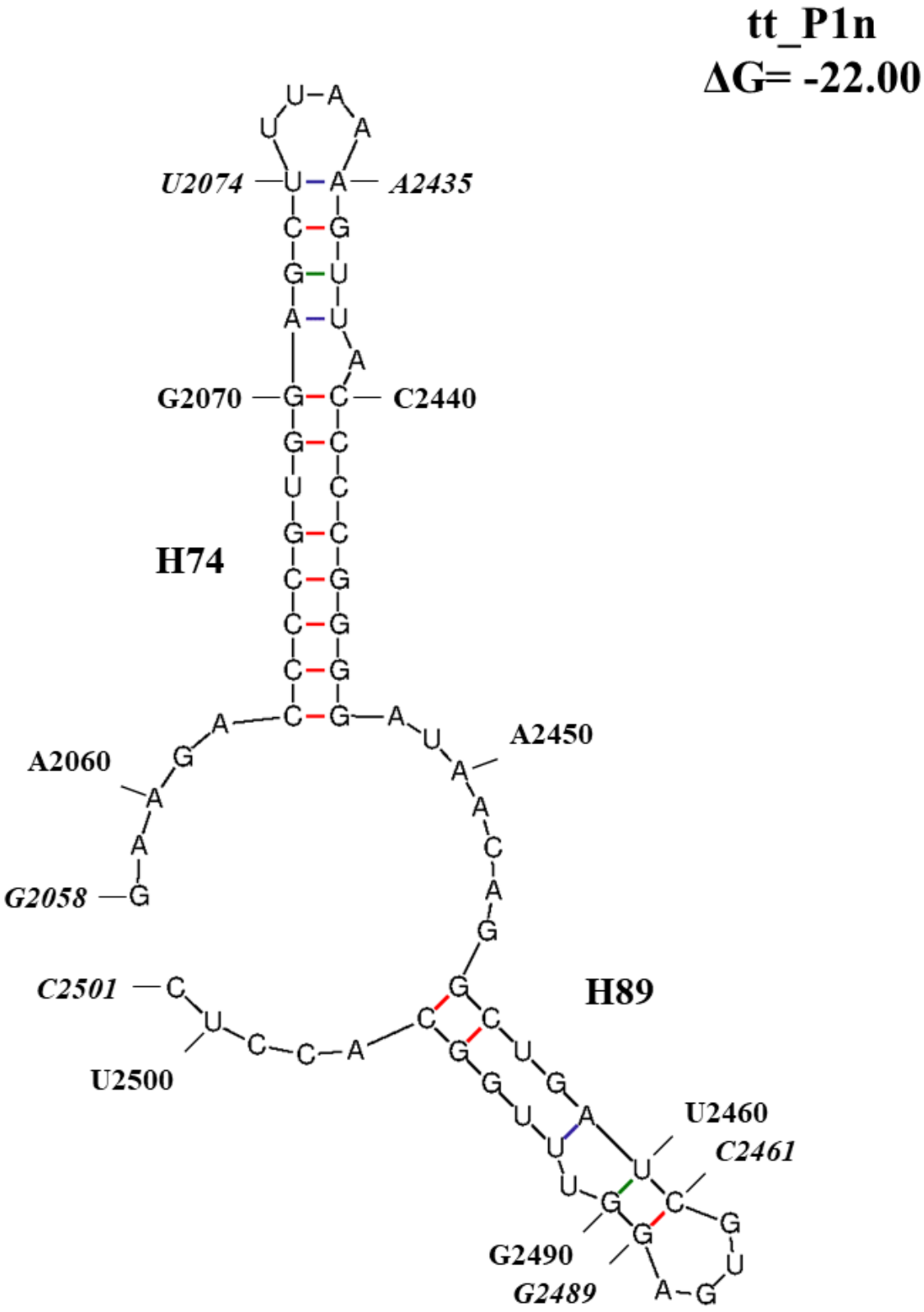
tt_P1n
ΔG= -22.00
U2074
A2435
G2070
C2440
H74
A2060
A2450
G2058
C2501
U2500
H89
U2460
C2461
G2490
G2489

Figure S18. Secondary structure of the tt_P1n construct predicted by mfold (Zuker, 2003). With a ΔG of -22.00 Kcal/mol. *Thermus thermophilus* numbering system is used. Shapes of H74 and H89 are the same as described in Figure S5. tt_P1c and tt_P1n differ in the replacement of 5′-CUUCGG-3′ by the 5′-UUAA-3′ as the closing element at the tip of H74. The implications of this change are discussed in the main text.

Figure S19

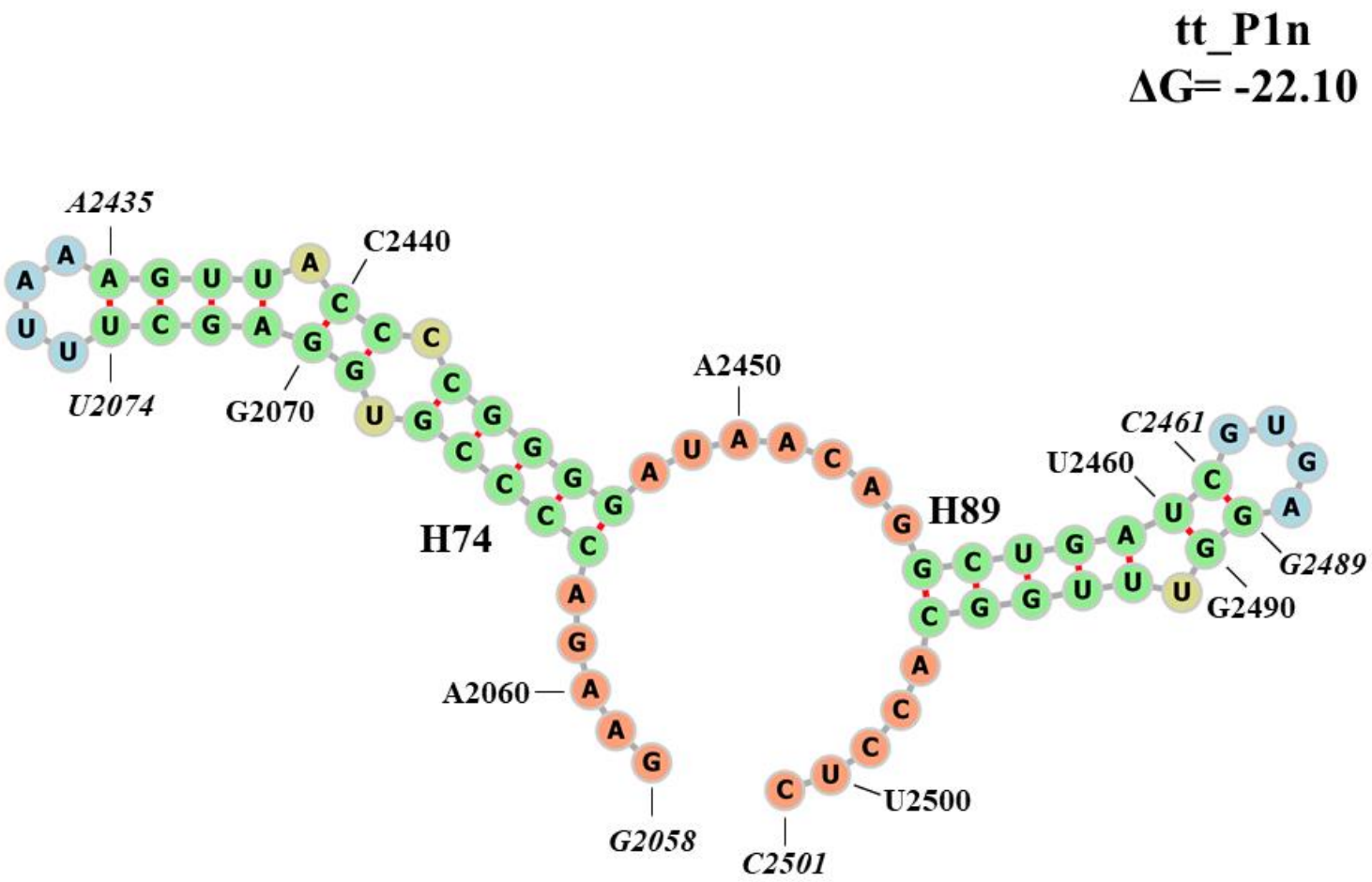
tt_P1n
ΔG= -22.10
A2435
C2440
U2074
G2070
A2450
C2461
U2460
H89
H74
G2489
G2490
A2060
G2058
U2500
C2501

Figure S19. Secondary structure of the tt_P1n construct predicted by RNAfold (Gruber *et al.*, 2008). With a ΔG of -22.10 Kcal/mol. *Thermus thermophilus* numbering system is used. Shapes of H74 and H89 are the same as described in Figure S5. tt_P1c and tt_P1n differ in the replacement of 5′-CUUCGG-3′ by the 5′-UUAA-3′ as closing element at the tip of H74. The implications of this change are discussed in the main text.

References

Bose, T., Fridkin, G., Davidovich, C., Krupkin, M., Dinger, N., Falkovich, A. H., … Yonath, A. (2022). Origin of life: protoribosome forms peptide bonds and links RNA and protein dominated worlds. *Nucleic Acids Research*, *50*(4), 1815–1828. DOI:10.1093/nar/gkac052

Gruber, A. R., Lorenz, R., Bernhart, S. H., Neubock, R., & Hofacker, I. L. (2008). The Vienna RNA Websuite. *Nucleic Acids Research*, *36*, W70–W74. DOI:10.1093/nar/gkn188

Leontis, N. B., & Westhof, E. (2001). Geometric nomenclature and classification of RNA base pairs. *RNA*, *7*(4), 499–512. DOI:10.1017/s1355838201002515

Lu, X.-J., Bussemaker, H. J., & Olson, W. K. (2015). DSSR: an integrated software tool for dissecting the spatial structure of RNA. *Nucleic Acids Research*, *43*(21), e142. DOI:10.1093/nar/gkv716

Rivas, M., & Fox, G. E. (2020). Further Characterization of the Pseudo-Symmetrical Ribosomal Region. *Life*, *10*(9), 201. DOI:10.3390/life10090201

Zuker, M. (2003). Mfold web server for nucleic acid folding and hybridization prediction. *Nucleic Acids Research*, *31*(13), 3406–3415. DOI:10.1093/nar/gkg595